

Eddington Capture Sphere around luminous stars

Adam Stahl¹, Maciek Wielgus²,
Marek Abramowicz^{1,3,4}, Włodek Kluźniak³, and Wenfei Yu⁵

¹ Physics Department, Gothenburg University, SE-412-96 Göteborg, Sweden

e-mail: gusstaad@student.gu.se

e-mail: marek.abramowicz@physics.gu.se

² Institute of Micromechanics and Photonics, ul. św. A. Boboli 8, PL-02-525, Warszawa, Poland

e-mail: maciek.wielgus@gmail.com

³ Copernicus Astronomical Center, ul. Bartycka 18, PL-00-716 Warszawa, Poland

e-mail: wlodek@camk.edu.pl

⁴ Institute of Physics, Faculty of Philosophy and Science, Silesian University in Opava, Bezručovo nám. 13, CZ-746-01 Opava, Czech Republic

⁵ Shanghai Astronomical Observatory 80 Nandan Road CN Shanghai 200030, China

e-mail: wenfei@shao.ac.cn

Received ????: accepted ????

ABSTRACT

Test particles infalling from infinity onto a compact spherical star with a mildly super-Eddington luminosity at its surface are typically trapped on the “Eddington Capture Sphere” and do not reach the surface of the star. The presence of a sphere on which radiation pressure balances gravity for static particles was first discovered some twenty five years ago. Subsequently, it was shown to be a capture sphere for particles in radial motion, and more recently also for particles in non-radial motion, in which the Poynting-Robertson radiation drag efficiently removes the orbital angular momentum of the particles, reducing it to zero. Here we develop this idea further, showing that “levitation” on the Eddington sphere (above the stellar surface) is a state of stable equilibrium, and discuss its implications for Hoyle-Lyttleton accretion onto a luminous star. When the Eddington sphere is present, the cross-section of a compact star for actual accretion is typically less than the geometrical cross-section πR^2 , direct infall onto the stellar surface only being possible for relativistic particles, with the required minimum particle velocity at infinity typically $\sim 1/2$ the speed of light. We further show that particles on typical trajectories in the vicinity of the stellar surface will also be trapped on the Eddington Capture Sphere.

Key words. Accretion – Stars: neutron – Gravitation – Radiation mechanisms: general – relativistic processes

1. Introduction

In Newtonian theory both gravity and radiative flux *in vacuo* diminish like $1/r^2$ with the distance from the center of the star. The luminosity in units of the Eddington luminosity, $L(r)/L_{\text{Edd}}$, at *any* distance from the star is equal to its value at the surface, $L(R)/L_{\text{Edd}}$, and is therefore *everywhere* either sub-Eddington, Eddington, or super-Eddington. However, in Einstein’s general relativity the radiative force diminishes more strongly with distance than the gravitational force, the redshifted luminosity $L(r)$ decreasing as $1/(1 - 2R_G/r)$, and a static balance of forces is achieved at that radius r at which $L(r) = L_{\text{Edd}}(1 - 2R_G/r)^{-1/2}$. For this reason, radiation may be super-Eddington close to the star, but sub-Eddington further away, reaching the Eddington value at the “Eddington Capture Sphere”, whose radius is (Phinney 1987)

$$R_{\text{Edd}} = \frac{2R_G}{1 - \left(1 - \frac{2R_G}{R}\right)^2 \left(\frac{L(R)}{L_{\text{Edd}}}\right)^2}. \quad (1)$$

At this radius the gravitational and radiative forces balance (for a static, optically thin hydrogen shell). The formula is in Schwarzschild coordinates, with the gravitational radius

R_G defined in Eq. (3). Abramowicz, Ellis & Lanza (1990) (hereafter AEL) have rigorously shown by analytic calculations that in the combined gravitational and isotropic radiation fields of a spherical, non-rotating, compact star, radially moving test particles (with proton mass, and Thomson cross-section for photon momentum absorption) are captured on this sphere and “levitate,” i.e., remain at rest.

Oh, Kim & Lee (2011) have shown that when the luminosity at the surface of the star is mildly super-Eddington, particles with non-zero orbital angular momentum can also be captured at R_{Edd} (see also Bini et al. 2009). This is because the Poynting-Robertson radiation drag acts as an effective torque, and for a wide class of trajectories reduces the orbital angular momentum to zero.

In this paper we further discuss the phenomenon of the Eddington Capture Sphere by considering two particular cases, one corresponding to initially quasi-circular motion close to the star, and the second being rather similar to the classic Hoyle & Lyttleton (1939) accretion model. We also consider the question of stability and speculate about possible astrophysical manifestations of the Eddington Capture Sphere.

All numerical results presented here were obtained with the Dormand-Prince method, which is a fourth-order ac-

curacy, adaptive step-size Runge-Kutta type integration method.

2. Equations of motion

We carry out all calculations in the Schwarzschild metric using standard Schwarzschild spherical coordinates,

$$\begin{aligned} t &= \text{time}, & r &= \text{radius}, \\ \theta &= \text{polar angle}, & \phi &= \text{azimuthal angle}, \end{aligned} \quad (2)$$

and extend the treatment of AEL to non-radial motion. Spherical symmetry of the problem assures that the trajectory of a test particle is confined to a single plane for any set of initial conditions. Without loss of generality, we assume that this is the equatorial plane $\theta = \pi/2$ in the Schwarzschild coordinates. Note that the stress-energy tensor of radiation $T^{(i)(k)}$ calculated in the stationary observer tetrad by AEL does not depend on the particle motion. Therefore, we may use here the AEL formulae for $T^{(i)(k)}$ with no change. We use dimensionless radius x , and dimensionless proper time τ defined by the scaling of the line element ds , as well as the dimensionless radius of the star, X ,

$$d\tau = \frac{ds}{R_G}, \quad x = \frac{r}{R_G}, \quad X = \frac{R}{R_G}, \quad \text{with } R_G = \frac{GM}{c^2}, \quad (3)$$

and introduce $B = 1 - 2/x$.

Assuming that the test particle is capturing momentum at a rate proportional to the radiative flux in its rest frame, thus suffering a rest-frame force of $(\sigma/c) \times \text{flux}$, the particle trajectory is described by two coupled, second order differential equations:

$$\begin{aligned} \frac{d^2x}{d\tau^2} &= \frac{k}{\pi I(R)X^2} \left(BT^{(r)(t)}v^t - [T^{(r)(r)} + \varepsilon] \frac{dx}{d\tau} \right) + \\ &+ (x-3) \left(\frac{d\phi}{d\tau} \right)^2 - \frac{1}{x^2}, \end{aligned} \quad (4)$$

$$\frac{d^2\phi}{d\tau^2} = -\frac{d\phi}{d\tau} \left(\frac{k}{\pi I(R)X^2} [T^{(\phi)(\phi)} + \varepsilon] + \frac{2}{x} \frac{dx}{d\tau} \right), \quad (5)$$

with the time component of the particle four velocity

$$v^t = B^{-\frac{1}{2}} \left[1 + B^{-1} \left(\frac{dx}{d\tau} \right)^2 + x^2 \left(\frac{d\phi}{d\tau} \right)^2 \right]^{\frac{1}{2}}, \quad (6)$$

and

$$\begin{aligned} \varepsilon &= BT^{(t)(t)}(v^t)^2 + B^{-1}T^{(r)(r)} \left(\frac{dx}{d\tau} \right)^2 \\ &+ x^2T^{(\phi)(\phi)} \left(\frac{d\phi}{d\tau} \right)^2 - 2T^{(r)(t)}v^t \frac{dx}{d\tau}. \end{aligned} \quad (7)$$

The parameter k is the surface luminosity in Eddington units,

$$k = \frac{L(R)}{L_{\text{Edd}}} = 4\pi^2 R^2 \frac{I(R)}{L_{\text{Edd}}}, \quad (8)$$

where $L_{\text{Edd}} = 4\pi GMm_p c/\sigma$.

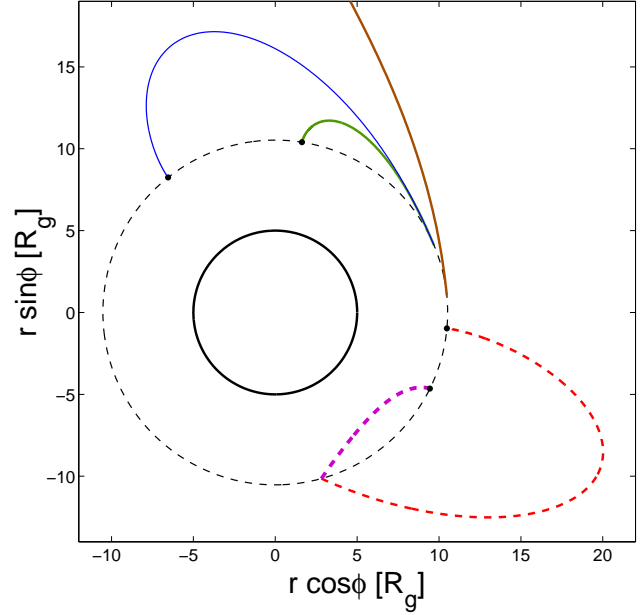


Fig. 1. Equilibrium on the Eddington Capture Sphere. Trajectories of particles returning to the Eddington sphere ($X = 5$, $k = 1.5$) are shown for four initial velocity perturbations: $v^\phi \equiv x d\phi/d\tau = 0.12$, $v^r \equiv dx/d\tau = 0$ (thick green continuous line), $v^\phi = 0.20$, $v^r = 0$ (thin blue continuous line), $v^\phi = 0.12$, $v^r = 0.10$ (thick red dashed line) and $v^\phi = 0.12$, $v^r = -0.10$ (extra thick violet dashed line). Also shown is a tangential escape trajectory (in thick brown) with initial $v^\phi = 0.32$, $v^r = 0$.

3. The capture sphere

The system of Eqs. (4), (5) allows a static solution $x(\tau) = x_{\text{Edd}}$ for

$$k = \left(1 - \frac{2}{x_{\text{Edd}}} \right)^{\frac{1}{2}} \left(1 - \frac{2}{X} \right)^{-1}, \quad (9)$$

where $x_{\text{Edd}} = R_{\text{Edd}}/R_G$, cf. Eq. (1). In the case of purely radial motion it was shown (AEL) that a critical point of nodal type is present at $x = x_{\text{Edd}}$, resulting in a stable equilibrium state of captured particles. A corresponding set of equilibrium points can be recognized in the system of Eqs. (4), (5). The set consists of points with $x = x_{\text{Edd}}$, and any value of ϕ and θ . (From Eq. [5] it follows that if $d\phi/dt = 0$, then $d^2\phi/dt^2 = 0$, and Eq. [4] reduces to the radial equation of AEL.) We refer to this set as the *Eddington Capture Sphere*. The radius of the sphere changes from $x_{\text{Edd}} = X$ to $x_{\text{Edd}} = \infty$ as k increases from $(1 - 2/X)^{-1/2}$ to $(1 - 2/X)^{-1}$.

4. Stability of equilibrium

Radial velocity perturbations were already discussed in AEL. In the case of general velocity perturbations, we observe stability in numerical experiments: if the azimuthal component of the velocity of a particle located on the capture sphere is slightly (or not so slightly) perturbed from zero value, the particle changes its location but returns to the stationary state somewhere else on the sphere. In this

sense, motionless “levitation” at a distance R_{Edd} from the star is a stable state. Such behavior is presented in Fig. 1 for $k = 1.50$, $X = 5.00$ (thick continuous black line), corresponding to $x_{\text{Edd}} = 10.5$ (thin dashed black line). We only show a small subset of the trajectories that we have computed, and for clarity we only show orbits with large initial velocity perturbations $\sim 0.1c$. For smaller perturbations the result is the same.

In fact, one can compute the minimum escape velocities from the Eddington Capture Sphere, these correspond to radial trajectories and are $v_{+}^r = 0.23$ for outward motion (escape to infinity) and $v_{-}^r = 0.51$ for inward motion (capture by the star), for the parameters considered. The minimum escape speed for trajectories tangent to the Eddington sphere (the second cosmic speed) is $v^{\phi} = 0.32$, the corresponding trajectory is also exhibited (in brown) in Fig. 1. One of the reasons for these unexpectedly large values of the escape velocities is the drag experienced by the particle even in purely radial motion.

5. Capture from circular orbits in the stellar vicinity

In the absence of radiation, a particle with appropriate angular momentum will follow a circular orbit around the star, but in a strong radiation field the particle will spiral inwards, since the radiation drag continuously removes angular momentum.

From Eq. (4), the azimuthal speed, v_{circ} , corresponding to a trajectory *initially* tangent to a circle, may be derived. Figure 2 shows some (non-escaping) trajectories ending on the Eddington sphere at $x_{\text{Edd}} = 10.5$ ($X = 5.00$, $k = 1.50$), for particles with an initial zero value of radial component velocity, $dx/d\tau(0) = 0$. Corresponding radial and angular velocity plots are presented in Fig. 3. The trajectory shown with a thin continuous red line starts at $x_0 = 15.0$ with $v^{\phi} = v_{\text{circ}} = 0.00344$. The thick dashed blue one and the thick continuous green one start at $x_0 = 8.00$ with $v^{\phi} = 0.00344$ and $v^{\phi} = 0.0300$, respectively. They are all (eventually) attracted to the Eddington capture sphere, and in the end the approach is almost radial due to the effective removal of all angular momentum by the radiation field.

6. Hoyle-Lyttleton accretion

We consider a situation resembling the model of a star moving through a uniform gas cloud, introduced by Hoyle & Lyttleton (1939). In this Section we take the star to have radius $X = 6$.

In Fig. 4, numerically calculated trajectories of incoming particles are shown. The parameters used were $k = 1.49$ (which implies $x_{\text{Edd}} = 151$), and the initial velocity at infinity $v_{\infty} = 5.00 \cdot 10^{-3}c$ (parallel to the x axis) for all particles. The initial value of $r \cos \phi$ was taken to be $-5000R_G$ and the impact parameters (initial $r \sin \phi$) of presented trajectories were taken from the set $\{0, 30R_G, 60R_G, \dots, 1500R_G\}$. Radial and angular components of velocity are presented in Fig. 5 for three selected particles, as a function of τ . The reduction of velocity along the trajectory is attributed to the influence of radiation, bringing the particles to a halt at $x = x_{\text{Edd}}$. Close to the equilibrium sphere, motion is almost radial and trajectories become perpendicular to the surface of the sphere.

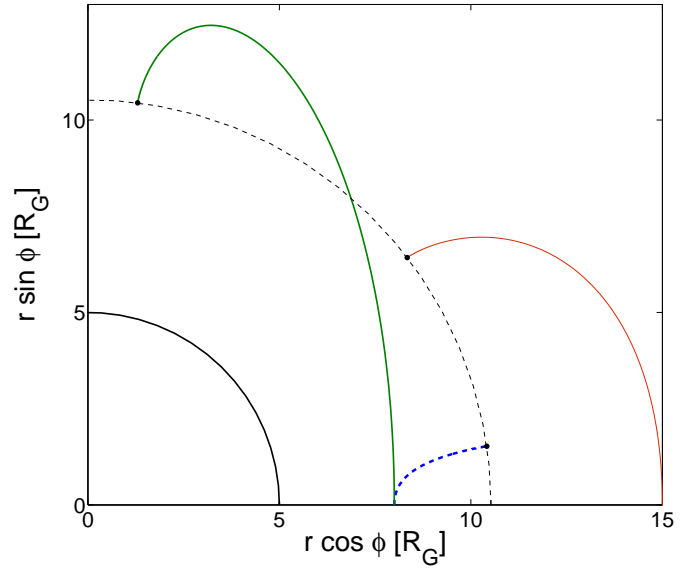


Fig. 2. Different trajectories for purely tangential initial velocity.

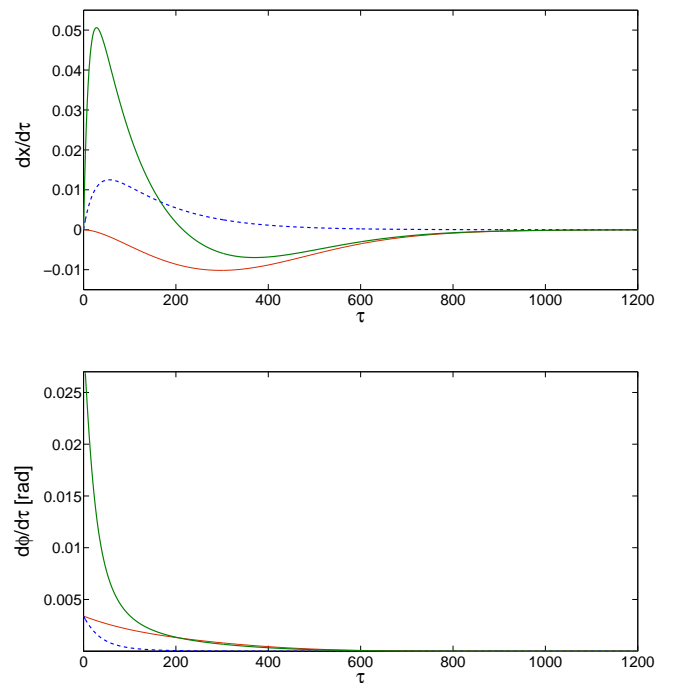


Fig. 3. Evolution of radial and angular velocity for trajectories in Fig. 2.

For a certain range of kinetic energies, the incoming particles can penetrate the capture sphere without reaching the stellar surface. Inside the sphere, radiation dominates over gravity and the particles will be pushed out until they reach the surface of the capture sphere again, and come to rest there. This is illustrated in Fig. 6, with the parameters chosen to be $v_{\infty} = 0.200c$, $X = 6.00$, $k = 1.45$, yielding $x_{\text{Edd}} = 30.5$. The initial value of $r \cos \phi$ was equal to $-2000R_G$ and the impact parameters of presented trajectories were taken from the set $\{0, 2R_G, 4R_G, \dots, 50R_G\}$.

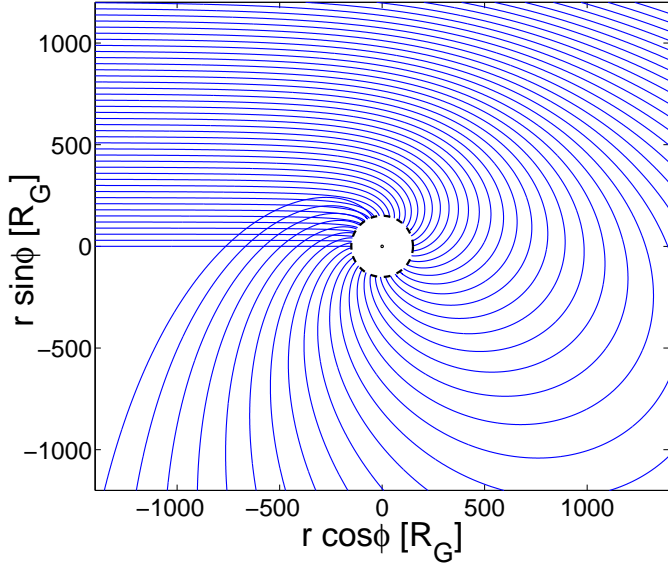


Fig. 4. The Hoyle-Lyttleton accretion problem for $X=6.00$, and $k=1.49$. The trajectories of particles for $v_\infty = 5 \cdot 10^{-3}c$, are shown. None of the test particles is accreted by the star, they are either trapped on the Eddington sphere or escape to infinity.

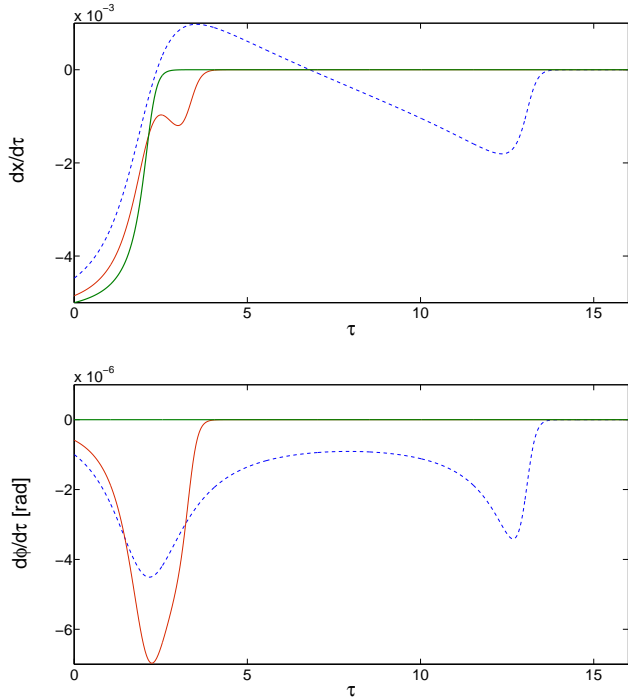


Fig. 5. Evolution of radial and angular velocity for three trajectories from Fig. 4 with impact parameter equal to 0 (thick continuous green), 500 (thin continuous red) and 1000 (dashed blue line).

The largest initial impact parameter of the captured particles was approximately equal to 1400 and 25.0 in the two presented cases (Fig. 4 and upper panel of Fig. 6), while the critical impact parameters of Hoyle-Lyttleton accretion in the absence of radiation would have been equal to 849 and 22.4, respectively. Critical trajectories separating the trajectories of escaping particles from the captured ones

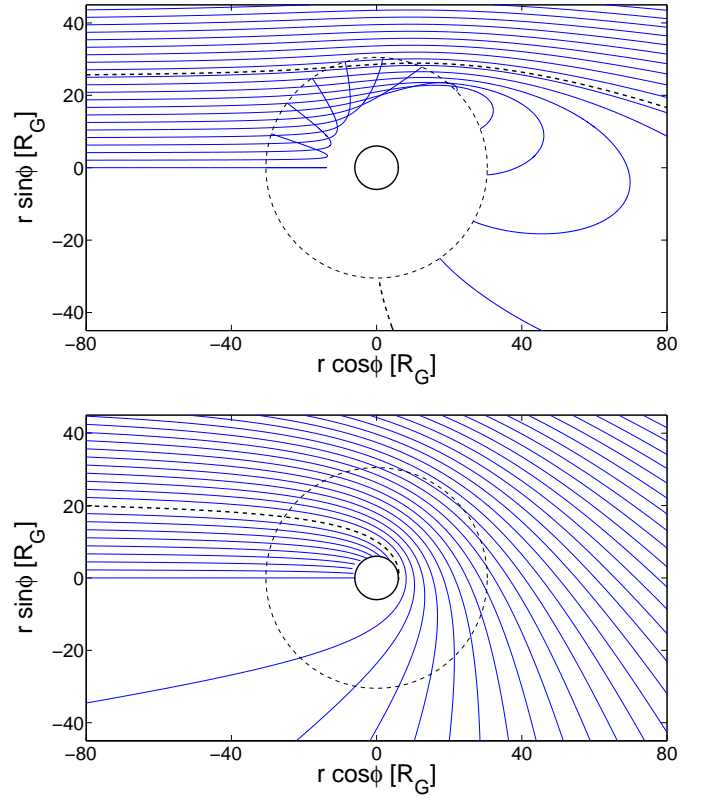


Fig. 6. Trajectories of particles for $v_\infty = 0.2c$ with (top, $k = 1.45$) and without (bottom, $k = 0$) radiation influence. The stellar surface is indicated by the inner circle (thick, continuous line), and the Eddington sphere by the dashed circle.

(impact parameters equal to 25.0 and 22.4) are drawn with thick dashed lines in the upper and lower panel, respectively, of Fig. 6.

As noted by Oh, Chun & Park (2012), in general, radiation drag is responsible for capturing particles from a larger area than in the case of accretion with no radiation. However, for the trajectories considered so far, no particle falls onto the surface of the star. For particles actually reaching the stellar surface, the converse statement is true, they come from a smaller cross-sectional area than in the case of accretion with no radiation, and in the cases considered here, smaller even than the cross-sectional area of the star πR^2 .

6.1. Direct capture onto the star

For a sufficiently low impact parameter, and a sufficiently high incoming velocity at infinity, a test particle may penetrate the Eddington sphere deeply enough to reach the stellar surface. The minimum value of v_∞ required to reach the star in the case corresponding to Fig. 4, i.e., $k = 1.49$ is shown as a function of the impact parameter in the top panel of Fig. 7 (the monotonically growing function depicted by the thick black line), for these velocities the particles settle on the stellar surface with zero velocity. This is a case of accretion not leading to any release of energy on the stellar surface. If the velocity at infinity is higher, the test particle will deposit some kinetic energy at impact on

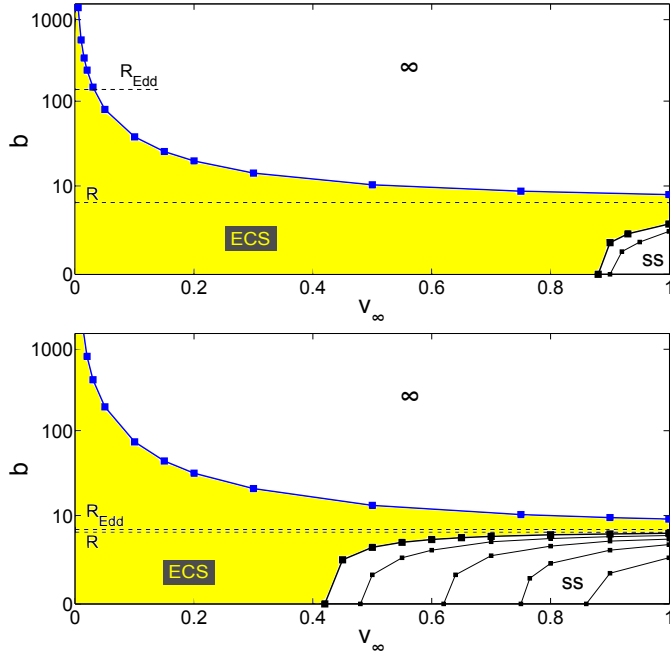


Fig. 7. Regions in the parameter space corresponding to escaping particles (region denoted by “ ∞ ” above the blue curve), particles ending up on the Eddington Capture Sphere (the shaded region between the thick black curve and the blue curve, denoted by “ECS”), and particles impacting the stellar surface (region below the thick black curve, denoted by “ss”), for two values of luminosity, $k = 1.49$ (top), and $k = 1.25$ (bottom). The radius of the star is $X=6$ for all plots in this Section. The impact parameter, b , is in units of R_G , and v_∞ in units of c . Particles with initial parameters on the thick black curve settle on the surface of the star with zero velocity. The thin black curves correspond to particles impacting with (from left to right): $v^r(R) = 0.05, 0.10, 0.15, 0.20$.

the stellar surface. However, the deposited kinetic energy will be a tiny fraction of the kinetic energy at infinity, as the impact velocities are much lower than v_∞ (thin black lines in Fig. 7). This outcome is just the opposite of what occurs when radiation drag and pressure may be neglected.

Other cases ($k = 1.45$, and $k = 1.25$) are illustrated in the bottom panel of Fig. 7 and in Fig. 8. The bottom panel of the latter figure illustrates the importance of radial radiation drag. The top curve illustrates the changing velocity of a test particle accelerated by gravity and decelerated by the radiation pressure [i.e., the term proportional to the $(t)(r)$ component of the stress tensor], but not suffering from radiation drag. The bottom curve shows the velocity computed with our full equations—clearly the resistance offered by the radiation field slows down the particle very effectively. Incidentally, the top curve illustrates another relativistic effect. For a rapidly moving particle the radiation pressure is enhanced by the ratio of $E/(mc^2)$ and it overwhelms the gravitational pull, so that the test particle is decelerated well outside the Eddington sphere.

7. Conclusions and discussion

We have shown that a luminous star in Schwarzschild metric can capture test particles from a wide class of orbits

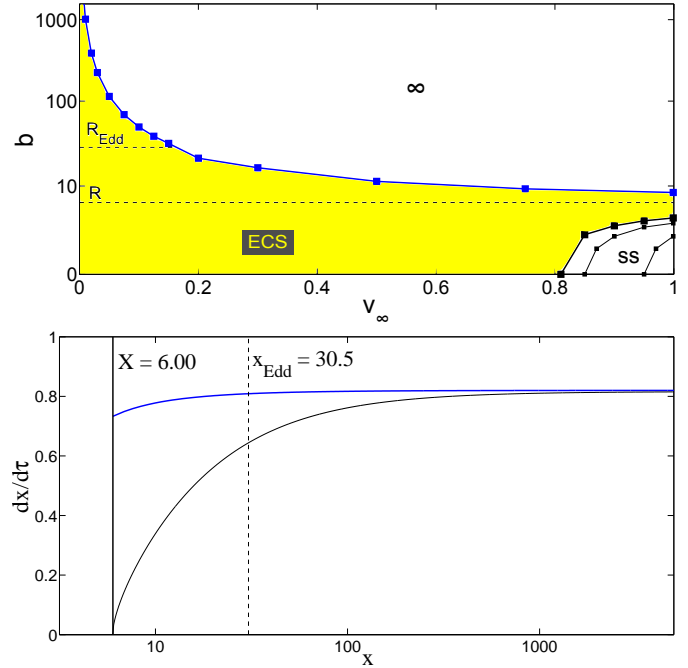


Fig. 8. The case of $k=1.45$. *Top:* Same as Fig. 7. *Bottom:* The velocity as a function of radius for radial infall ($b = 0$) and $v_\infty = 0.82c$, with and without radiation drag (bottom and top curves, respectively).

onto a spherical surface of radius larger than the star itself. The particles come to rest on this sphere, because radiation drag eventually removes all of their angular momentum, as shown by Oh, Kim, & Lee (2011). The particles remain suspended above the surface of the star, because every point on the capture sphere corresponds to a position of equilibrium, the equilibrium being stable in the radial direction (Abramowicz, Ellis, Lanza 1990) and neutral in directions tangent to the sphere. The radius of this “Eddington Capture Sphere” depends on the ratio of the stellar luminosity to the Eddington luminosity (Eq. [1]). Thus, accreting compact stars, as well as stars which eject matter, may be surrounded by a shell of matter at rest, as long as the luminosity of the star is close to the Eddington luminosity (super-Eddington on the stellar surface).

The trajectories of particles falling from infinity in the gravitational field of a mildly super-Eddington compact star were investigated in Section 6. We showed that radiation drag strongly reduces both the azimuthal and the radial component of test particle velocities. This leads to a moderate enhancement of the capture cross-section by the Eddington sphere, relative to the cross-section for accretion by a non-radiating star, and a drastic suppression of the cross-section for actual accretion onto the stellar surface. Radiation drag also leads to a dramatic decrease in the kinetic energy deposited at the surface.

It is interesting to speculate that the presence of the Eddington Capture Sphere, an effect of Einstein’s general relativity, may play a role in the formation and ejection of shells of matter by massive stars in the final stages of their evolution, such as Wolf-Rayet stars, or the luminous blue variables (LBV stars). In principle, the capture sphere can exist at any radius outside the star, if the stellar luminosity has the appropriate value. However, the larger the radius of the sphere (in units of the Schwarzschild radius),

the more finely tuned the luminosity has to be—for a $10R_G$ (5 Schwarzschild radii) capture sphere the luminosity at infinity has to be $0.95L_{\text{Edd}}$, while for a $500\,000 R_G$ sphere the luminosity has to be equal to the Eddington value to an accuracy better than one part in a million. While our discussion was couched in terms of the Thomson scattering cross-section, similar results will hold if other scattering or absorption processes contribute to momentum transfer from the radiation field to the particles. The capture sphere is located at that radius at which radiation pressure on matter at rest balances the gravitational pull of the star. Outside the sphere, the radiation pressure is too weak to balance gravity, inside the sphere it overcomes the gravitational pull.

It is expected that a more likely application of the Eddington capture sphere will be found in the interpretation of the behaviour of accreting neutron stars in low mass X-ray binaries. In particular, in the Z sources, the inner radius inferred from both the kHz QPOs and the accretion-disk spectral component have been determined to vary rapidly at a luminosity which is thought to be close to the Eddington value (Yu, van der Klis, & Yonker, 2001, Lin, Remillard, & Homan, 2009). In particular, the kHz QPOs vary with the normal branch oscillation (NBO) phase, which may indicate radiation induced rapid drifts of the innermost accretion flow. Perhaps these findings could be understood in terms of the expected behaviour of accreting matter accumulating on (a sector of) the Eddington sphere. In the non-spherical geometry of accretion disks, radiation scattered in non-radial directions can escape from the system. Therefore the accreting fluid can “levitate” above the star only as long as it is optically thin. As more and more matter accumulates at the capture radius of Eq. (1), the shell eventually becomes optically thick and the outer layers of the fluid outweigh the radiation pressure support, leading to rapid accretion of matter and to the consequent evacuation of the region near the Eddington capture sphere, allowing the process of accumulation to begin again. One would also expect the accreting fluid to be spread out to higher altitudes (lower and higher values of the polar angle θ) than those subtended by the inner parts of the optically thick disk, as the incoming fluid forms a “puddle” on the surface of the Eddington capture sphere. A more detailed understanding of actual behaviour of Z sources would require relaxing the assumption of spherical symmetry, on which all the calculations in this paper were based. Comparison of the theoretical expectations with the observed NBO and its related flaring branch oscillation (FBO) would be very interesting.

In the atoll sources, which are less luminous, the Eddington luminosity is attained during X-ray bursts. It would be worthwhile to investigate whether the Eddington capture sphere plays a role in the evolution of “radius expansion bursts” (e.g., Damen et al. 1990). In addition, in the persistent emission at rather high luminosity levels $\sim 0.4L_{\text{Edd}}$, a ~ 7 Hz QPO similar to the NBO in the Z sources was also observed in the atoll source 4U 1820-30 (Wijnands, van der Klis, & Rijkhorst, 1999). The effect we are considering above is global, but may apply to local properties of the accretion flow as well.

8. Acknowledgements

We thank Saul Rappaport for discussion and for providing test orbits against which our codes were checked. Research supported in part by Polish NCN grants NN203381436 and UMO-2011/01/B/ST9/05439, as well as by a Swedish VR grant. Research in the Institute of Physics at the Silesian University in Opava supported by the Czech grant MSM 4781305903. WK acknowledges the support of the National Science Foundation and the hospitality of the Aspen Center in Physics, where a part of this work was completed.

References

- Abramowicz, M.A., Ellis, G.F.R. & Lanza, A., 1990, ApJ 361, 470
- Damen, E., *et al.*, 1990, A&A 237, 103
- Bini, D., Jantzen, R.T., Stella, L., 2009, Class. Q. Grav. 26, 055009
- Hoyle, F., Lyttleton, R.A., 1939, Proc. Camb. Phil. Soc. 35, 405
- Lin, D., Remillard, R.A., & Homan, J., 2009, ApJ 696, 1257
- Oh, J.S., Kim, H., & Lee, H.M., 2011, New A. 16, 3, 183
- Oh, J.S., Chun, M.Y., & Park, Ch., 2012, Gen. Relat. Grav., in press
- Phinney, E.S., 1987, in *Superluminal Radio Sources*, ed. J.A. Zensus and T.J. Pearson (Cambridge: Cambridge University Press), p. 12.
- Wijnands, R., van der Klis, M., Rijkhorst, E.-J., 1999, ApJ 512, L39
- Yu, W., van der Klis, M., Jonker, P.G., 2001, ApJ 559, L29